Silicon Photoelectrodes Prepared by Low-Cost Wet Methods for Solar Photoelectrocatalysis

Bruno Fabre, Gabriel Loget

Silicon Photoelectrodes

Prepared by Low-cost Wet Methods

for Solar Photoelectrocatalysis

Bruno Fabre,[a,]* *Gabriel Loget*[a,]*

[a]CNRS, ISCR (Institut des Sciences Chimiques de Rennes)-UMR6226, Univ Rennes, Rennes F-35000, France

*Email: bruno.fabre@univ-rennes1.fr

*Email: gabriel.loget@univ-rennes1.fr

CONSPECTUS

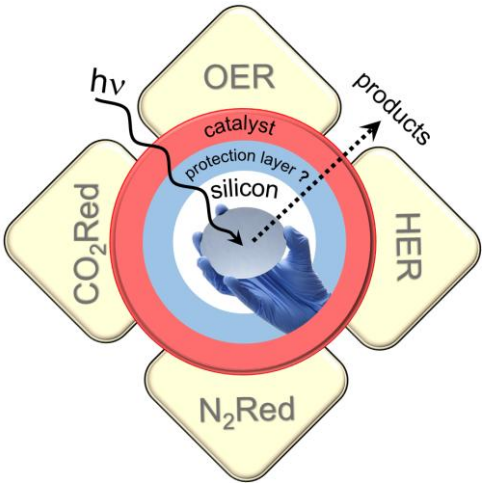

The electrochemical conversion of sunlight by photoelectrochemical cells (PECs) is based on semiconductor electrodes that are interfaced with a liquid electrolyte. This approach is highly promising, first, because it can be employed for the generation of a chemical fuel (e.g., H_2) to store solar energy that can be used on-demand to generate electricity when the sun is not available. Second, it can be seen as a concept reminiscent of photosynthesis, where CO_2 is converted into a valuable feedstock by solar energy. Thus, photoelectrochemical cells are sometimes referred to as "artificial leaves". Silicon, being the main semiconductor in the electronics and photovoltaic sector, is a prime candidate to be used as the light absorber and the substrate for building photoelectrochemical cells. However, Si alone has "poor-to-no photoelectrochemical performance". This is caused by its weak electrocatalytic activity for cathodic reactions (namely, the hydrogen evolution reaction (HER), the CO_2 reduction reaction (CDRR), and the N_2 reduction reaction) and by its deactivation in the anodic regime, prohibiting its use for the oxygen evolution reaction (OER). This latter reaction is essential for supplying electrons to generate a solar fuel. Due to these problems, layers that both protect and are catalytically active are typically employed on Si photoelectrodes, but require rather sophisticated manufacturing processes (e.g., atomic layer or electron beam deposition), which hinders research and innovation in this field. Nevertheless, our group and others have demonstrated that these layers are not always required and that highly active and stable Si-based photoelectrodes can be manufactured using simple wet processes, such as drop casting, electroless deposition, or aqueous electrodeposition. In this Account, we first introduce the topic and the possible structures that can be easily obtained starting from commercial Si wafers. Then, we discuss strategies that have been employed to manufacture photocathodes based on p-type Si. Among these, we describe Si photocathodes coated with metal, inorganic compounds such as metal sulfides as well as more original constructs, such as those based on macromolecules composed of a catalytic Mo_3S_4 core and a polyoxometallate macrocycle.

Also, we discuss the elaboration and the advantages of Si photocathodes obtained by grafting organometallic catalysts which are promising candidates for reaching excellent selectivity for CDRR. Then, the manufacturing of photoanodes based on n-Si is reviewed with an emphasis on those prepared by electrodeposition of a transition metal such as Ni and Fe. The effect of the catalyst morphology, density, and Si structuration is discussed, future developments are proposed.

1. Introduction and Scope

The development of efficient, low-cost and robust electrocatalytic interfaces able to carry out the electrochemical water splitting into dihydrogen H_2 and dioxygen O_2 under harsh conditions is still nowadays challenging. In this field of electrocatalysis, the use of photoactive semiconducting electrodes instead of non-photoactive conventional conducting ones (carbon and metallic electrodes) as catalyst immobilization could provide a real benefit in terms of energy gain because it allows the electrochemical process to be activated by sunlight with photogenerated charge carriers. As a result, the electrocatalytic reaction at illuminated modified n-type or p-type semiconductors is often observed at less positive or negative potentials, respectively, compared to the case of similarly modified conducting electrodes. This beneficial potential shift is called photovoltage (V_{oc}). Among the semiconductors used for this goal, silicon with its small bandgap of 1.1 eV has appeared as one of the most promising candidates because of its abundance, its ability to harvest photons from a large portion of the solar spectrum and the favorable position of its conduction band edge relatively to the H^+/H_2 redox potential for HER (**Figure 1a**).[1] Also interestingly in the context of the electrochemical conversion of CO_2 to high-added value products, its bandgap encompasses the different proton-assisted multielectron reduction potentials for CO_2. Thus, the interfacing of Si with an appropriate deposited catalyst should *a priori* enable these two technologically important electrochemical reactions to be achieved at high rate. So, modified p-type Si photocathodes have been demonstrated to be effective for acid HER (**Reaction 1**) and CDRR. Huge efforts have been put by chemists for the development of Earth-abundant noble metal-free catalysts with the hope of reaching an HER activity comparable to that of the archetypical platinum. Molecular catalysts are also particularly appealing for tuning the selectivity of an electrocatalytic reaction that can lead to different electrogenerated products, such as CDRR. Regarding OER (**Reaction 2**), the interfacing of n-type Si surfaces with

catalysts to prepare efficient and robust photoanodes is much more intricate than that for Si photocathodes essentially owing to its anodic degradation. Consequently, the effective and convenient protection of n-Si with, e. g., a thin metal oxide layer is often required to access operational photoanodes.

$$4\ H^+(aq) + 4\ e^-_{Si} \rightarrow 2\ H_2(g) \qquad (1)$$

$$4\ OH^-(aq) + 4\ h^+_{Si} \rightarrow O_2(g) + 2\ H_2O(l) \qquad (2)$$

Emphasis will be placed on simple, low-cost and reliable methods to deposit both the catalyst and the protection layer on Si. The advantages of wet methods such as drop-casting, spin-coating, electroless deposition and aqueous electrodeposition over vacuum-based physical methods are that they allow a photoelectrode preparation through simple and fast protocols and they can be performed by most laboratories. Accordingly, they will be more particularly scrutinized in this Account. In contrast, lithography-based patterning and atomic layer deposition (ALD) techniques, reactive ion etching (RIE) and more generally all costly physical methods using high-vacuum conditions, pump and cooling system, are beyond the scope of this Account. Also, the introduction of pn^+ or np^+ homojunction (buried junctions) using the thermal diffusion of doping elements through Si or ion implantation will not be tackled here even though such an approach is powerful and relevant to increase the photovoltage of the resulting p-type Si photocathode or n-type photoanode.

Apart from catalyst and interface engineering considerations, silicon surface textures have been also introduced to enhance the light absorption by silicon, to improve the collection efficiency of photogenerated minority charge carriers and to increase the electrochemically active surface area, with respect to planar silicon. In this respect, only silicon texturing using wet methods and involving low cost reagents and basic equipment will be considered in this Account. Typical structures prepared using such conditions are shown in **Figure 1b-d** and

include Si nanowires (Si NWs, **Figure 1b**), vertically aligned Si needles (referred to black Si (BSi), **Figure 1c**), and Si micropyramids (SimPy, **Figure 1d**).

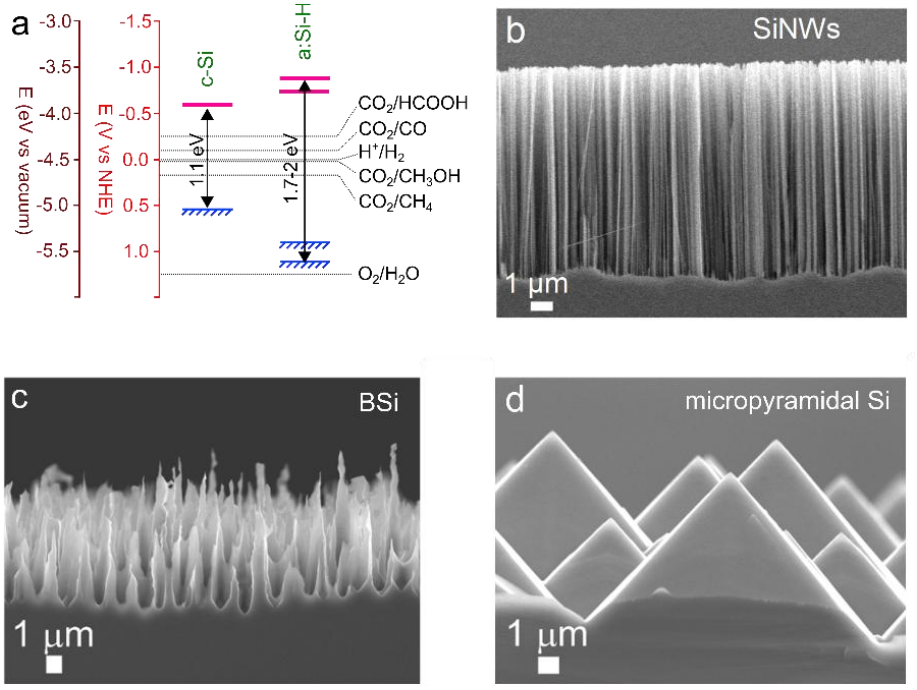

Figure 1. a) Scheme presenting the relative positions of the band edges of crystalline Si (c-Si) and amorphous Si (a-Si:H) with respect to the standard potentials of the important redox couples for water splitting and CO_2 reduction. b-d) Silicon surface structures used for preparing catalyst-modified photoelectrodes: b) Si nanowires (SiNWs), Reproduced with permission from ref [2]. Copyright 2015 American Chemical Society; c) black Si (BSi), Reproduced with permission from ref [3]. Copyright 2019 American Chemical Society and d) Si micropyramidal array (SimPy), Reproduced with permission from ref [4]. Copyright 2020 Wiley-VCH.

The interested reader who wishes to go deeper into the subject is invited by the authors to read the Supporting Information that contains an extended version of the Introduction section enriched by additional references.

2. Si Photocathodes

2.1. Typical photocathode structures

In contrast with Si photoanodes, the protection step is less critical for Si photocathodes because the formation of silicon oxides is disfavored under reductive conditions and in strongly acid media which are often used for HER. The situation is somewhat different when p-type Si is used in alkaline solution for which Si dissolution is significant, following **Reaction 3**[5] and proper protection is required for developing stable and high-performance p-Si photocathodes.

$$Si(s) + 2\ OH^-(aq) + 2\ H_2O(l) \rightarrow SiO_2(OH)_2^{2-}(aq) + 2\ H_2(g) \qquad (3)$$

Efficient and stable p-type Si photocathodes prepared by low-cost wet methods usually consist of a metal-insulator-semiconductor (MIS) structure with an ultrathin (~1-2 nm) silicon oxide layer separating the Si surface from the chemically or (photo)electrochemically deposited metal present as isolated nanoparticles/islands or conformal film (**Figure 2**).[1] For the latter, the resulting photocathode yields often limited photocurrent output when illuminated from the frontside owing to the parasitic light absorption/reflection by the metallic layer. Besides MIS structures, hybrid metal ion-based molecular catalyst-Si interfaces have also been tested for solar photoelectrocatalysis taking advantages of the chemical specificity and the redox tunability of molecular catalysts to control the selectivity of the targeted electrocatalytic reaction. In that case, the catalytic component consists of a monolayer, multilayer, or a polymer film.

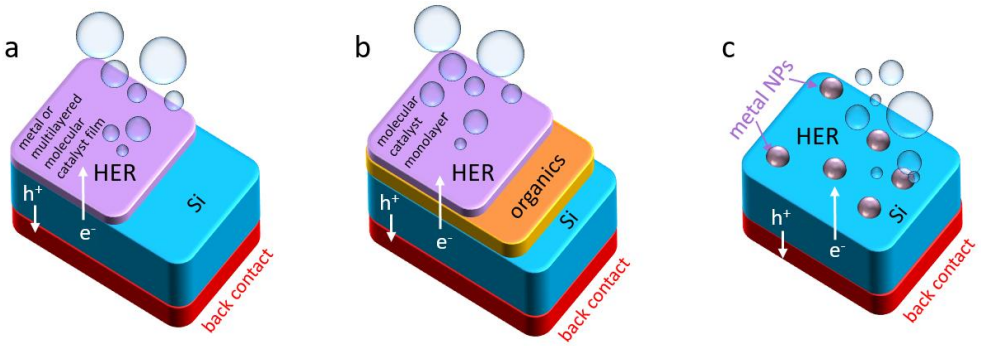

Figure 2. Typical structures used for Si photocathodes integrating a) a metal or multilayered molecular catalyst film, b) molecular catalyst monolayer with "organics" being the organic chain bridging the catalyst to Si and c) isolated metal NPs. Note that SiO_x, present at the Si interface is not represented here.

2.2. Inhomogeneous metal-based coatings on photocathodes

The two most commonly used low-cost and wet methods for coating a silicon photocathode with a metal catalyst are the electroless and (photo)electrochemical depositions. The electroless deposition of metallic nanoparticles (NPs) onto semiconducting surfaces by galvanic displacement occurs spontaneously if the redox potential of the employed metal couple (M^{n+}/M^0) is higher than those of both the Si surface and the hydrogen evolution.[6] So, the spontaneous deposition of metals (Au, Pt and Ag) onto p-type hydrogen-terminated Si(100) or Si(111) (Si:H) yielded catalytically active photocathodes with strongly attached metal catalyst. In contrast, for metallic couples with lower redox potentials, photoelectrodeposition was favored with the aim of producing metal NPs-modified photocathodes with comparable intimate Si/metal contacts. Besides electro- and electroless deposition methods, drop-casting and spin-coating are also considered as alternative simple and low-cost approaches.

2.2.1. (Semi-) Noble metals

The integration of Pt onto p-type Si has been motivated for boosting photoelectrochemical HER.[7] So, planar p-type Si(100) and Si(111) photocathodes covered with electrolessly

deposited Pt NPs exhibited good performance metrics for HER in acid conditions, testified by ca. 300 mV photovoltages and short-circuit photocurrent densities j_{sc} at 0 V (all potentials in this article are referred vs Reversible Hydrogen Electrode (RHE)) exceeding 20 mA cm^{-2} under simulated sunlight.[8,9] When the planar Si was replaced by a Si NWs array, the resulting Pt NPs/SiNW photocathode exhibited a ~100 mV-enhanced photovoltage as a result of the orthogonalization of light absorption and charge-carrier collection.[10] It is worth noticing that Pt deposited by physical vapor deposition yielded photocathodes with very low photovoltages. Such differences were ascribed to the presence of a thin interfacial SiO_x layer between silicon and the metal NPs in the case of electrolessly deposited Pt.[9] Moreover, in another report, it has been demonstrated that both the morphology and the density of the Pt NPs deposited on Si(100) can be fine-tuned by the electroless deposition temperature and time.[11] The formation of multifaceted isolated Pt islands and nanotrenches in the Si bulk was found to be beneficial for improving the catalytic performance of the photoelectrodes for HER.

Besides Pt and Au, the electroless deposition of semi-noble Ag NPs on p-type Si(100) led to photocathodes showing photoelectrocatalytic activities for the multi-electron reduction of CO_2 to CO[12,13] and N_2 to NH_3.[14] Indeed, the conduction band of Si is relatively well positioned for the photogenerated electrons to promote efficiently these two electrochemical reduction reactions of interest (**Figure 1a**). In the first example, the combination between Ag NPs, and a photoactive silicon surface afforded high-performance photocathodes which were capable of photoelectrochemically reducing CO_2 to CO with an onset potential of 0 V.[12] Such a synergistic effect was also observed for the photoelectrocatalytic reduction of N_2 to NH_3 with a BSi/Ag photocathode that yielded a high Faradaic efficiency of about 55% at −0.1 V.[14]

2.2.2. Other metals

Planar, SimPy, and Si NWs derivatized with photoelectrochemically, electrolessly or drop-casted Ni-[8,15] and Mo[16–18]-based catalysts have demonstrated high catalytic efficiency for sunlight-driven HER in strongly or weakly acid media. In particular, planar Si(100) decorated with Ni NPs showed remarkable performance metrics for HER, such as an onset potential V_{oc} of 0.34 V and j_{sc} of 10.0 mA cm^{-2},[8] which could be even improved for nickel phosphide $Ni_{12}P_5$ NPs deposited on Si NWs.[15] Mo-based complexes, such as MoS_x,[16] $Mo_3S_4^{4+}$,[17] and MoO_x[18] (**Figure 3a,b**), have also been explored as HER catalysts. The $\{Mo_3S_4\}$ core, identified as one of the most promising MoS_x-based HER electrocatalysts, has been covalently associated to a polyoxotungstate electron/proton sponge moiety. It produced a striking synergistic effect featured by high HER performance and enhanced stability in operation for the resulting photocathodes (**Figure 3c-e**).[19,20] Furthermore, the use of a conjugated polymer film as the catalyst-embedding matrix appeared as a promising and scalable approach to retain durably the active phase on the silicon photocathode.[20] Besides HER, a great attention has been paid to metal-modified Si(100) photocathodes for the CO_2 reduction. In particular, photocathodes modified with Bi[21,22] and Sn[23] nanostructures have been considered for the photoelectrocatalytic conversion of CO_2 to formate with the first ones showing superior performance (**Figure 3f,g**).

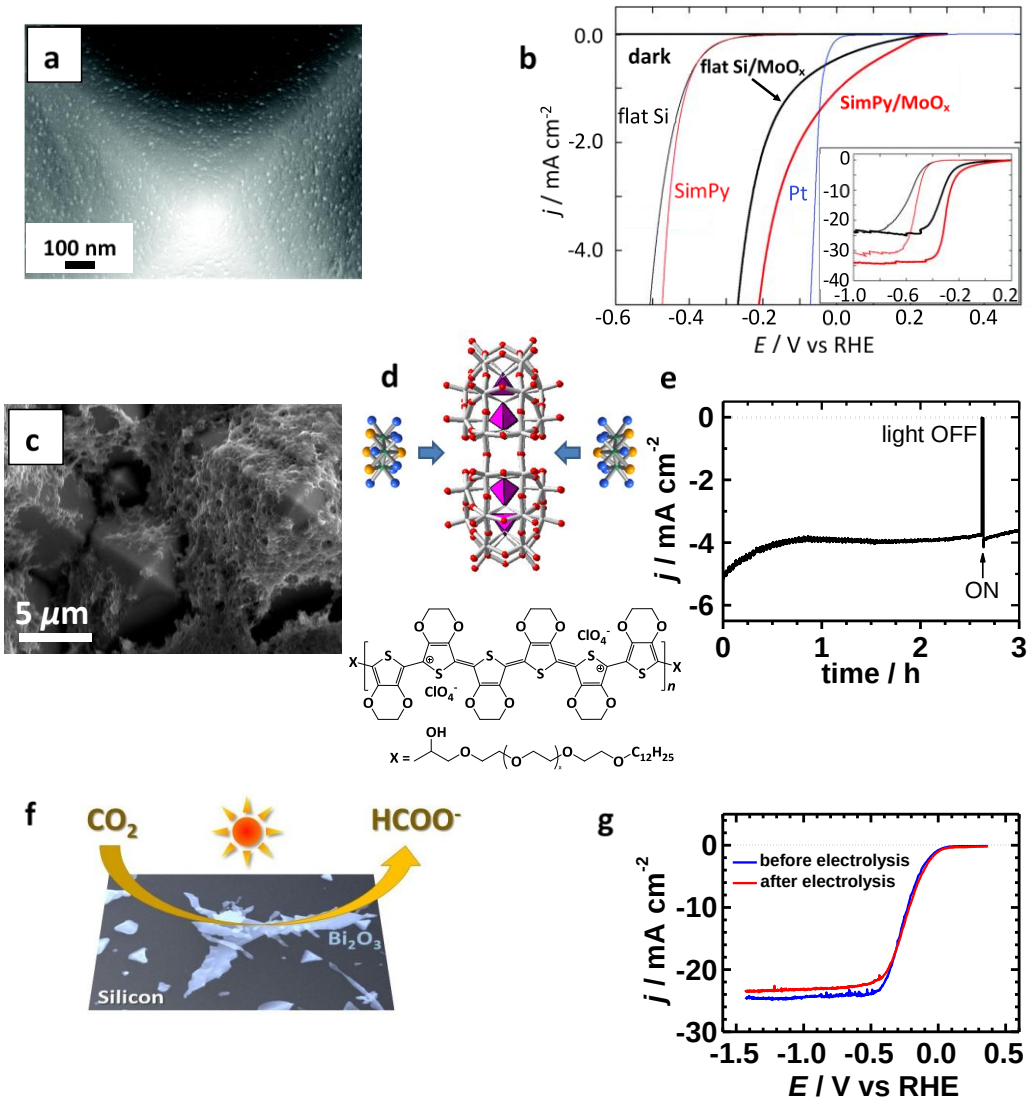

Figure 3. a) Top view SEM of SimPy after electroless deposition of MoO_x NPs and b) linear sweep voltammograms (LSVs) at pH 1 under simulated sunlight: bare flat Si(100):H (black thin line), bare SimPy:H (red thin line), MoO_x-decorated flat Si(100) (black thick line) and MoO_x-decorated SimPy (red thick line). Inset: LSVs showing the behaviour of the Si photocathodes at more negative potentials. Reprinted with permission from ref [18]. Copyright 2017 Royal Society of Chemistry. c) SEM image of the polyoxothiometalate (thio-POM)/poly(3,4-ethylenedioxythiophene) PEDOT-coated SimPy for solar-driven HER. d) Schematic view of the thio-POM resulting from the covalent association of $[Mo_3S_4(H_2O)_9]^{4+}$ cluster with the macrocyclic polyoxotungstate $[H_7P_8W_{48}O_{184}]^{33-}$, and PEDOT used as the catalyst-embedding polymer matrix. e) Photocurrent density-time curve obtained during the potentiostatic electrolysis at 0 V using the thio-POM-functionalized photocathode under simulated sunlight at pH 0.3. Reprinted with permission from ref [20]. Copyright 2019 American Chemical Society. f) Photoelectrocatalytic reduction of CO_2 to formate from electrodeposited Bi_2O_3 nanostructures-modified Si(100) photocathodes and g) LSVs at 20 mV s^{-1} of the photocathode before and after 30 min electrolysis at -1.03 V in CO_2-saturated 0.5 M $KHCO_3$ solution. Reprinted with permission from ref [22]. Copyright 2020 Wiley-VCH.

2.3. Covalently grafted molecular electrocatalysts

The integration of molecular complexes of metals on Si photocathodes has been much less explored. Despite several potential constraints inherent to this strategy (e.g., multistep synthetic procedures, hydrophobicity and possible degradation of the complexes), the immobilized molecular catalysts can offer some advantages, such as the control/tunability of the selectivity of the electrocatalytic reaction through the ligand and metal design, and the protection of the underlying Si surface. Although the selectivity criterion is not crucial for HER, it becomes paramount for multielectron and multiproton electrochemical processes such as CDRR for which numerous carbon related products may be electrogenerated. Nevertheless, while some non-noble metal (e.g. Mn, Ni or Fe)-based molecular complexes immobilized on carbon substrates have enabled a fine control of the electrochemical reduction of CO_2 to H_2, CO or formic acid, examples of selectivity tuning for CDRR using molecular catalyst-modified Si photocathodes have not been reported to date.

Monolayers of Ni^{II} [24,25] or Co^{III} [26] complexes have been immobilized on flat Si(111):H or BSi:H surfaces through a covalent organic linkage or π-π interactions with a preassembled aromatic monolayer, respectively (**Figure 4**). The resulting Ni- and Co-modified photocathodes showed V_{oc} for solar-driven HER of 0.07 V in CH_3CN medium containing a trifluoroacetic acid-based proton source[25] and -0.20 V in 0.1 M H_2SO_4 solution,[26] respectively, with photocurrent densities exceeding 20 mA cm^{-2}. Besides HER kinetic aspects, these studies provided crucial information on how to design hybrid semiconductor/molecule architectures to maximize the catalytic activity of the photocathodes. More precisely, the semiconductor band bending must be maximized first before considering the kinetic effects provided by the attached molecular complex. In this frame, the band bending may be modulated by both magnitude and orientation of interfacial dipoles generated by the attached molecule. Successful strategies to maximize band bending include the manipulation of either

the spatial environment of the metallic center when it is covalently bound to Si[25] or the electronic coupling between Si and the catalyst when it is noncovalently attached through π-π interactions.[26] Compared with catalytic monolayers, organometallic polymer films deposited on Si can provide some benefits in terms of higher surface coverage of the catalyst and enhanced protection of Si. A Ni complex-modified Si(100) photocathode was prepared from the casting of a mixture of a Ni^{II} complex salt and Nafion polymer as a cation-exchanging binder.[27] Another approach employed the electropolymerization of a pyrrole monomer *N*-substituted by a Mn^{I} 2,2'-bipyridine complex to decorate SiNWs photocathodes with a organometallic polymer film covering homogeneously the sidewalls of SiNWs (**Figure 4e**).[2] Consistent with what was observed in homogeneous catalysis with the dissolved complex, the hybrid photocathodes operated durably for sunlight-assisted CO_2-to-CO reduction with quantitative conversion yield (**Figure 4f**).

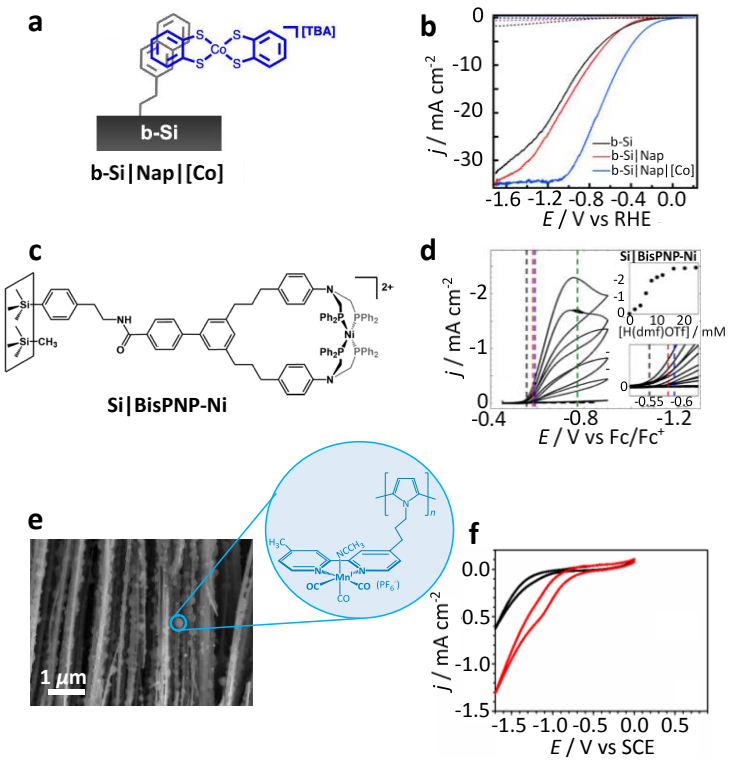

Figure 4. a) Immobilization of the Co^{III} bis(benzenedithiolate) complex on black Si through π-π interactions with preassembled naphthalene monolayer. b) LSVs of the unmodified, naphthalene- and Co-modified black Si photocathodes in 0.1 M H_2SO_4 under simulated sunlight. The dashed lines correspond to the response in the dark. Reprinted with permission

from ref [26]. Copyright 2020 American Chemical Society. c) Ni^{II} complex-/methyl-terminated mixed monolayer covalently bound to Si(111):H surfaces. d) CVs of the Ni(II) complex-modified Si(111) photocathode in CH_3CN + 0.2 M $LiClO_4$ under 33 mW cm^{-2} light intensity, with the addition of increasing concentration of a proton source. Reprinted with permission from ref [25]. Copyright 2020 American Chemical Society. e) SEM image of SiNWs:H after electrodeposition of a Mn^{I} complex-substituted polypyrrole film and f) CVs of the electrocatalytic Mn–based polymeric film deposited onto SiNWs:H in the dark (black line) and under 20 mW cm^{-2} light intensity (red line) in CO_2-saturated CH_3CN + 0.1 M Bu_4NClO_4 + 5% v/v H_2O. Reprinted with permission from ref [2]. Copyright 2015 American Chemical Society.

3. Si Photoanodes

3.1. Typical photoanode structures

As shown in **Figure 1a**, the valence band edges for crystalline Si (c-Si) and amorphous Si (a-Si:H) are located at higher energy than that corresponding to the standard potential of the O_2/H_2O redox couple. This means that Si cannot spontaneously oxidize water without the application of a consequent external bias. Thus, at a first sight, Si is not the best candidate to be used as an absorber for the design of monolithic water splitting PECs. It is, however, important to realize that many photovoltaic Si homojunctions and heterojunctions can be produced. These systems can be used as photoelectrodes, improving the reachable V_{oc} compared to what is possible with a simple Si/electrolyte junction or a Si/metal junction.[28] Besides, because of Si's ubiquity in the industry and its lowering price, it is reasonable to think that if an H_2-producing PEC technology emerges in the future, it could be based on Si. It is thus important to develop Si-based photoanodes through strategies that can be later adapted to more elaborate crystalline or thin-film Si-based junctions. In addition, as many semiconductors share similar characteristics to Si (such as its instability), this material can also be considered as a model for the development of preparation strategies that could be adapted to other semiconductor systems.

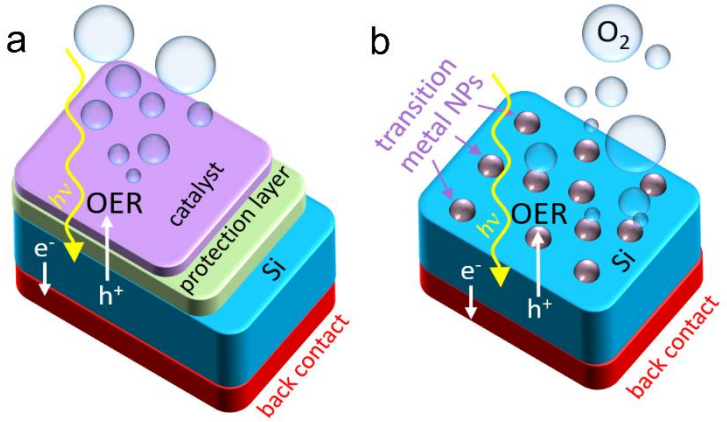

Figure 5. a) Typical structure used for Si photoanodes. b) Structure of a Si photoanode inhomogeneously modified with transition metal nanoparticles. Note that SiO_x, present at the Si interface is not represented here.

A straightforward way to develop Si-based photoanodes is to use commercially available photoactive moderately doped monocrystalline n-type Si (n-Si). Manufacturing Si-based photoanodes for performing oxygen evolution reaction (OER, **Reaction 2)** has been a considerable challenge because of the instability of Si. In the field of OER, general interest is given to strongly alkaline electrolytes because they allow employing inexpensive materials (e.g., Ni, Co, or Mn) as efficient electrocatalysts.[29] This is the first problem for Si because it spontaneously decomposes at these pH through alkaline etching (**Reaction 3**). This reaction is an issue in the frame of water splitting as it can induce the decomposition of immersed Si electrodes at the open circuit potential. The second deactivation mechanism is the oxidation of Si that generates an insulating Si oxide onto the surface. Oxidation is highly favorable thermodynamically, occurs spontaneously upon exposure to air, and is more pronounced when Si is used as an anode. The formation of this passive oxide prohibits charge transfer at the Si/liquid interface and inhibits the activity of Si photoanodes. For that reason, typical Si-based photoanodes (**Figure 5a**) consist of the Si absorber, a protection layer, and a catalytic layer.[30] The role of the first layer is to prevent the aforementioned decomposition mechanisms by physically separating the Si absorber from the electrolyte. Typical protection layers consist

of a dense and conformal layer of a metal oxide, deposited by a physical vapor deposition process, such as ALD.[30] The role of the second layer is to grant sufficient activity for the oxidation reaction, typically, homogeneous or inhomogeneous coatings based on Ni or Co.[1,31–33] A particularly interesting architecture for OER is the MIS.[34] In this arrangement, the Si surface is composed of a few nm-thick insulating layer comprised of SiO_x and another dielectric (ALD TiO_2, HfO_2, or Al_2O_3) coated by a catalytic transition metal. In many examples, the protection and the catalytic features are combined in a single layer[35,36] deposited by physical deposition. Such structures imply that important considerations are fulfilled by the layers in terms of conductivity, light absorption, and band energetics to allow optimal operation of the photoanode. A crucial challenge in this field lies in combining activity, stability, and low processing cost of the Si-based photoanode. Two remarkable pioneering reports must be mentioned in this Account because they allowed envisioning a drastic simplification of the photoanode's architecture. The first one reports on the impressive effect of few nm-thick Ni metal thin films deposited on n-Si(100) surface for operating OER at pH 14 for 12 h.[37] The other one shows that Co particles electrodeposited on n-Si(100) can promote OER at pH 14 for ~2 h.[38]

3.2. Inhomogeneous coatings of electrodeposited transition metals

In 2017, we reported that aqueous electrodeposition of randomly-dispersed Ni NPs on n-Si(100), as shown in **Figure 6a**, can be used to manufacture photoanodes that promote simulated sunlight-driven OER at pH ~14 for 10 h at around 30 mA cm^{-2}.[39] These photoanodes and those modified with other transition metal NPs can be considered as inhomogeneous MIS junctions composed of nanoscale n-Si/SiO_x/metal junctions (**Figure 6b**).[38,39] Under illumination, photogenerated holes flow to the metal NPs and reach the solid/liquid interface to trigger OER (**Figure 6c,d**). An activation process, which occurs when these photoanodes are cycled by voltammetry, induces considerable improvement of the OER

kinetics (**Figure 6d**).[40] Surface analyses revealed that this is caused by the formation of a $Ni(OH)_2$/NiOOH catalytic shell (doped by adventitious Fe) around the Ni NPs, which is known to have a high activity for OER.[41] Because of their fundamental difference from conventional Si-based photoanodes covered by homogeneous thin films (**Figure 5, inset of Figure 6d**), the stability of these photoanodes is particularly intriguing. It has been shown that the photoanode deactivation is caused by the removal of the Ni NPs from the Si surface.[40] It is hard to know if the NPs detachment is related to bubble generation or slow dissolution during the electrolysis, however, electron microscopy reveals that the Si surface does not undergo severe alkaline etching. This is in good agreement with an anodic protection mechanism where the Si regions that are uncoated by Ni (in contact with the electrolyte) are protected by an anodic oxide (SiO_x), which is also evidenced by voltammetry recorded at bare n-Si(100).[40] This is quite interesting because the anodic SiO_x formation, which is usually considered as a drawback for Si-based photoanode (detrimental to conductivity), has a beneficial role here by providing Si protection. The effect of the metal coverage (controlled by the electrodeposition charge) on the photoelectrode performance was studied by our group[39] and others.[38,42–46] In all cases, it was reported that an increase in Ni coverage induces a gain in stability but also a loss in photoelectrochemical performance. First, light absorbed by Si is considerably decreased for thick Ni layers, which, in turn, lowers the limiting photocurrent densities. In addition, the onset potential for OER was found to be strongly dependent on the Ni coverage, with better performance obtained at low coverage, due to an increased photovoltage.[39,42–45] Other approaches have been then explored to prepare similar photoanodes, such as pulsed electrodeposition,[42] electroless plating,[44,47] and two-step electrodeposition.[48,49] Electrodeposition of Ni NPs can also be used as a step in the preparation process to make more elaborate junctions.[50,51] Later, Oh *et al.* reported the extension of the strategy to another transition metal, Fe, which was obtained by a similar electrodeposition process.[4]

Comparatively, these electrodes are less stable than the Ni ones (a few hours at pH~14) but their stability can be considerably improved (up to more than five days) when using a K^+/Li^+ borate buffer solution at pH 9.6.[4] It can be hypothesized that this electrolyte inhibits the volume expansion of the $Fe(OH)_2$ phase[37] and that the lower pH helps promoting photoanode integrity by decreasing the etching of Si and SiO_x.[4] If these results show that electrolyte composition can have a beneficial effect on the photoelectrode stability, one has to keep in mind that it is highly important to maintain a pH alkaline enough to avoid dissolution of the transition metal NPs during anodic polarization.

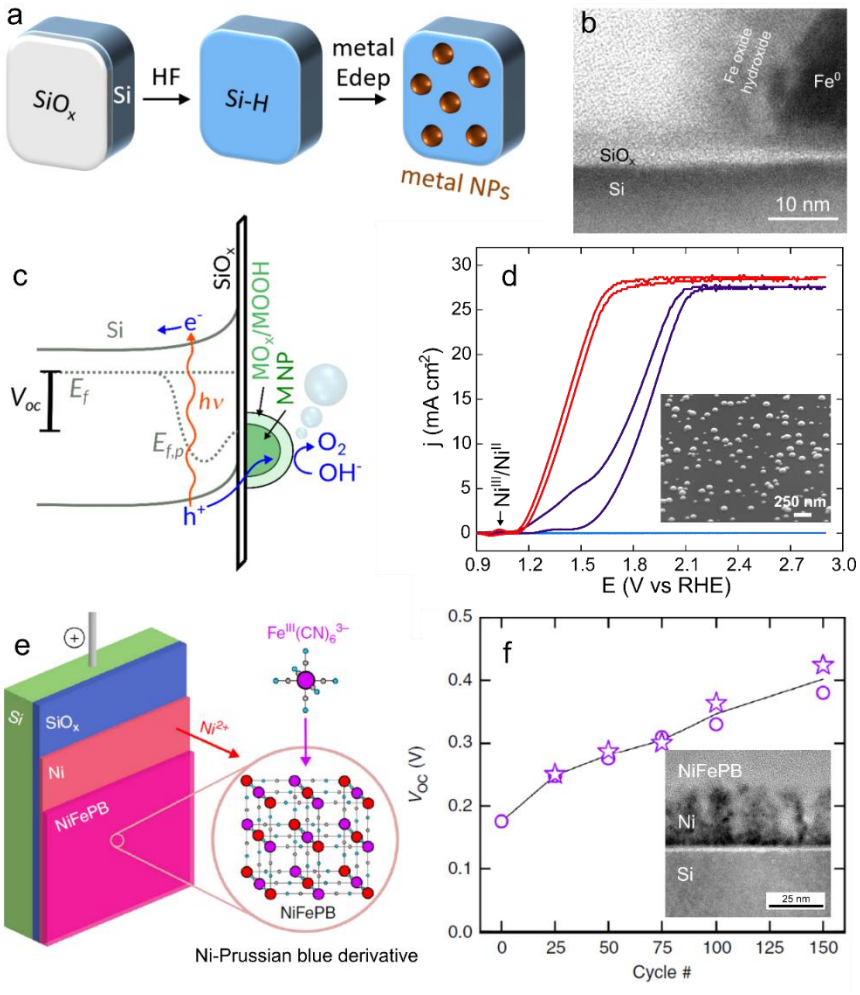

Figure 6. a) Scheme showing the steps employed for preparing Si-based photoanodes by electrodeposition of transition metal NPs. b) High-resolution TEM image showing the n-Si/SiO_x/Fe interface on a photoanode prepared by Fe electrodeposition on n-Si. Reproduced with permission from ref [4]. Copyright 2020 Wiley-VCH. c) Schematic band diagram of an n-Si/metal (M = Fe, Co, and Ni) photoanode during OER. d) Cyclic voltammograms (1 M

NaOH) recorded in the dark (blue) and under simulated sunlight before (purple) and after (red) photoelectrochemical activation (100 cyclic voltammetry scans) of a photoanode manufactured by Ni electrodeposition on n-Si. e) Scheme showing the electrodissolution method employed for manufacturing the $Si/SiO_x/Ni/NiFePB$ surfaces. f) V_{oc} measured on n-$Si/SiO_x/Ni/NiFePB$ as a function of the number of electrodissolution cycles. Inset: TEM images of a $Si/SiO_x/Ni/NiFePB$ surface. Reproduced with permission from ref [52]. Copyright 2019 Springer-Verlag.

The photoanodes made by electrodepositing Ni[39] or Fe[4] share many features with those obtained by electrodepositing Co,[38] namely: their inhomogeneous nature, the formation of a catalytic oxyhydroxide phase under operation, and the improvement of the photoelectrochemical performance for lower surface coverage. It is worth noting that the last feature is also observed in the case of (initially) homogeneous nm-thick Ni layers deposited by electron beam,[37] and such similarities can be attributed to the inhomogeneous nature of these electrodes in operation.[53] The n-Si-based photoanodes prepared by electrodepositing dispersed metal NPs, are, by nature, quite different from the typically employed photoelectrodes which are generally considered highly homogeneous solid/liquid junctions (**Figure 5a,b**), such as classical semiconductor/electrolyte junctions, or solid/solid junctions.[54] Their main structural difference originates from their inhomogeneity. Indeed, the surface of the semiconductor is in contact with more than one phase and, at first sight, several interfaces may impact the properties of the junction. Specifically, in the case of Ni-coated photoanodes, n-Si/SiO_x, as well as its interface with the electrolyte, Ni, $Ni(OH)_2$, NiO_x, and NiOOH phases junctions could play an important role in the overall response of the electrode. These photoanodes also show unusual properties, the first one being their photovoltage that can exceed 0.4 V,[39,55] which is far much higher than what is expected for their conformal n-Si/Ni counterparts. Indeed, because of Fermi level pinning, which typically occurs at semiconductor/metal junctions, the typical Schottky barrier for n-Si/Ni conformal junctions is rather small. Due to the structural complexity of the photoanode, it has been so far difficult to determine precisely the origin of these high photovoltages. According to recent works, this

phenomenon is caused by the formation of a silicide layer[56] or the suppression of electron current caused by the SiO_x interlayer.[55] Besides, the so-called "pinch-off effect", i.e., the screening of low barrier regions occurring under a critical size regime,[54,57,58] has also been used by several groups to explain these surprisingly high photovoltages. In these models, the low barrier region is n-Si/Ni,[45] and the high barrier region is n-Si/SiO_x,[53] n-Si/NiOOH,[45] or n-Si/NiO_x,[42] depending on the reference. If the elucidation of the photoanode behavior is still far from being fully understood, the advantage of this electrodeposition-based method is undeniably its simplicity. Indeed, it only requires a potentiostat to produce Si-based photoanodes that can be studied over for several hours or days.

3.3. Electrodissolution of homogeneous transition metal coatings

Experiments performed with Si photoanodes produced via metal electrodeposition showed that higher performance (photovoltage and photocurrent) is associated with low surface coverage and higher inhomogeneity of the transition metal on n-Si. As all these electrodes were prepared using a similar electrodeposition method, we later wished to verify if this behavior was also observed for differently produced photoanodes. Towards that goal, we used metal electrodissolution. The conceptual idea was to start with a homogeneous and conformal transition layer covering n-Si(100) (a 25 nm-thick Ni film) and to increase the junction inhomogeneity by dissolving the metal layer in a controlled fashion (**Figure 6e**).[52] n-Si/SiO_x/Ni MIS photoanodes were used as starting substrates, in which the SiO_x layer is thin enough (~1.5 nm) to enable charge tunneling from Si to Ni. Electrodissolution is particularly interesting because, in addition to dissolving the Ni layer, it can be employed to simultaneously modify the junction with a redox-active species, which can be employed to probe the V_{oc} of the photoanode.[52] To do so, the Si/SiO_x/Ni MIS electrodes were directly modified by electrochemically oxidizing the Ni layer in an acidic solution in the presence of $Fe(CN)_6^{3-}$. Ni^0 is thus converted into soluble Ni^{2+}, which coordinates with the cyano groups of

$Fe(CN)_6^{3-}$ to generate an electroactive Ni-Prussian blue (PB) derivative (NiFePB) coating the solid interface (inset of **Figure 6f**). The number of anodic cycles allows controlling to which extent the Ni thin film is dissolved, thus, its degree of inhomogeneity. A study of the photovoltage as a function of the electrodissolution (**Figure 6f**) revealed that the performance followed the same trend as for the electrodeposited metals, namely, photovoltage and photocurrent are improved when the inhomogeneity of the Ni thin film is increased.[52] In addition to that, increasing the density of catalytic sites by the porosification enhances the kinetics of the electrocatalytic reaction. Later, this electrodissolution/redox functionalization approach was investigated for depositing different PB derivatives (NiRuPB and CoFePB) on n-Si(100) photoanodes initially coated by Ni and Co thin films.[59] These electrodes were employed for photoelectrocatalyzing OER and the urea oxidation reaction, both at pH ~14.[52,59] In these conditions, the PB derivative is etched from the surface and the metal oxyhydroxide formed *operando* is the catalytically active species, as discussed previously in the case of photoanodes prepared by electrodeposition.[40,41] In addition to the electrodissolution approach that has been discussed in this section, it is interesting to note that other anodic processes have been reported to make high-performance Si-based electrodes. For instance, anodic precipitation[28] and anodization[60] have been employed on protected thin-film Si solar cells to improve their OER activity.

3.4. Control over the Si structure and the catalyst geometry

Nanostructuring semiconductor electrodes is a usual way to enhance light absorption and charge carrier collection efficiency. Because carrier diffusion in Si is long enough to ensure efficient collection, nanostructured or textured Si is mainly explored to increase photon absorption. To assess the versatility of our preparation strategies on different n-Si substrates and to determine if the photoanodes performance could be further improved by enhanced photon absorption, the electrodeposition of transition metals was investigated on structured Si

absorbers.[3] BSi, composed of an array of highly-absorbing Si spikes prepared via a simple wet procedure (**Figure 1c**),[5] was used as the electrode substrate. It was modified by electrodepositing Ni-NiFe core-shell NPs (**Figure 7a**) by a two-step electrodeposition method. The NiFe shell layer was chosen because the oxidation products of NiFe alloys ($Ni_{1-x}Fe_xOOH$) are known to be among the best OER catalysts.[41] The so produced photoanodes promoted OER for more than 15 h at pH ~14,[3] showing that electrodeposited NPs are effective on different types of Si. However, using this specific substrate did not allow to improve the performance compared to that obtained on planar Si(100) and exhibited rather low external quantum efficiencies. This indicates that, despite their strong absorption properties, these substrates are not optimal for OER. Another structured Si surface made of SimPy structures (**Figure 1d**) prepared by alkaline etching (**Reaction 3**), was modified by electrodeposition of Fe NPs (**Figure 7b**).[4] Although the optical absorption of these substrates is much lower than BSi discussed before, they are made of very smooth Si(111) facets, which is very different from the Si spikes constituting BSi surfaces that likely own a high density of surface defects. Overall, SimPy/Fe photoanodes provided better performance, with respect to their planar (100) counterparts as demonstrated by cyclic voltammetry and external quantum efficiency measurements.[4] This was already the case in another example involving p-type Si(100)-based photocathodes for HER.[18] This considerable performance improvement originates from the enhanced absorption of photons which are converted to holes and employed effectively for the OER reaction. The results obtained on both types of structured Si show clearly how structured and absorbing SC absorbers can affect photoelectrochemical performance. If structuration is beneficial for light absorption, it often increases the defect surface density and is not always associated with better photoelectrochemical properties. It is primordial to ensure that the structuration does not impede with the absorber property.

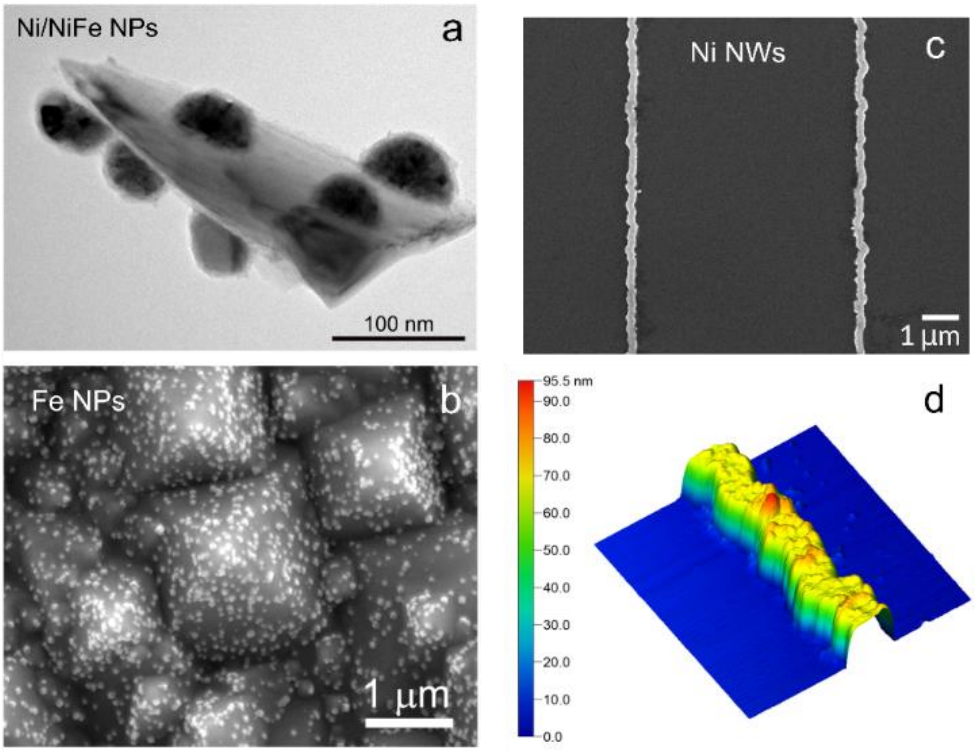

Figure 7. a) TEM picture showing a single Si spike detached from the BSi surface after electrodeposition. Reproduced with permission from ref [3]. Copyright 2019 American Chemical Society. b) Top-view SEM image showing the Fe NPs on Si micropyramidal array (SimPy). Reproduced with permission from ref [4]. Copyright 2020 Wiley-VCH. c) Top view SEM image of Ni NWs electrodeposited on n-Si(100). d) AFM picture (2×2 µm^2) of one Ni NW electrodeposited on n-Si(100). Reproduced with permission from ref [61]. Copyright 2021 Royal Society of Chemistry.

In addition to the absorber structure, the structure of the transition metal NPs is also expected to affect the properties of photoanodes. Using classical electrodeposition methods such as that previously described does not allow fine control over the NP morphology and their respective spacing. For that reason, a templated electrodeposition method based on the lithographically patterned nanowire electrodeposition (LPNE) method[62] was implemented to deposit transition metal nanowires (NWs) onto n-Si(100), as shown in **Figure 7c,d**.[61] This method allows for manufacturing tailored photoanodes by electrodeposition, with fine control over the geometrical parameters of the metal catalysts (Ni or Co NWs). The OER performance of Ni NWs-modified photoanodes having different morphological features and pitches was rationalized by a qualitative simulation approach, which revealed the importance

of the SiO_x layer and suggested the existence of a high barrier region originating from the contact between n-Si and a metal oxide or oxyhydroxide phase on the NWs.

4. Conclusions and overview of future developments

We have presented recent developments in the preparation and the study of Si-based photoelectrodes. Overall, we can observe similarities in architectures for photocathodes and photoanodes. In general, protection interlayers are placed between the catalysts and Si to prevent (to some extent) Si from degradation mechanisms. If these layers can extend the lifetime of a photoelectrode up to months, we have discussed that such layers are not always required and that stability of several days can be reached without physical vapor deposition methods. This is particularly true for photocathodes that are relatively stable in operation but also in the case of photoanodes when the thin SiO_x layer, generated *in situ*, does not impede hole transfer from the Si to the catalyst. However, in this case, it is important to properly evaluate the stability domain of the photoelectrode and be aware that degradation can be more pronounced under open circuit conditions or in the dark.

At the outermost surface, the presence of a specific catalyst is essential to sustain electrochemical activity. The choice of this catalyst depends on the target reaction as well as the operation conditions (electrolyte composition, pH, applied potential), which will dictate not only the catalyst efficiency but also its stability. Pourbaix diagrams are, in this regard, particularly useful to properly choose appropriate catalysts. Catalysts have been deposited on Si in the form of dispersed islands or conformal homogeneous coatings, and sometimes the effect of these two morphologies on the photoelectrocatalysis has been studied. In this respect, in recent works on n-Si photoanodes for OER, nanosized catalyst islands have been demonstrated to be highly beneficial with respect to conformal thin films, inducing a higher photovoltage. In addition to metals or metal hydroxides catalysts that can be deposited on Si substrates by simple and low-cost methods, inorganic metal-based compounds such as

phosphides, sulfides, molecular clusters, or hybrid entities can also be immobilized onto the Si surface and used for photoelectrocatalysis. Simple immobilization strategies are diverse, ranging from drop-casting to incorporation into matrices such as conducting polymers. In the latter case, precautions should be taken if the relatively thick matrix absorbs visible light to maintain a sufficiently high photocurrent density.

The immobilization of organometallic molecular catalysts (through non-covalent or covalent linkage) is also a rather simple method which is particularly interesting for conferring a high degree of selectivity, as required for CDRR. While the synthesis of the organometallic molecular catalysts usually requires knowledge and skills in organic chemistry, their interfacing with Si is relatively straightforward through Si:H surface chemistry.[1,63]

The strength of these simple methods is that they can open this important field of research to many groups, which may induce stimulation and promote creativity in the field of photoelectrochemistry. The low-cost modification processes can sometimes be coupled with more elaborated structuration or patterning techniques to reveal their operating mechanisms. Considerable progress has been made, as testified by the fact that these photoelectrodes have been used for unassisted photoelectrochemical solar water splitting (without potentiostat).[51,64] However, at the moment, it seems still challenging to prepare Si-based photoelectrodes that can be used for months without employing physical vapor deposition methods. Degradation mechanisms are multiple and can originate from Si or the deposited coating, and differ depending on the experimental conditions. To illustrate this, we report herein three examples of potential failure mechanisms that can occur at photoanodes: *i*) local pH drop may lead to the dissolution of a Ni or Fe-based catalyst during OER operation; *ii*) the protecting SiO_x layer may be dissolved by hydroxides at the open circuit condition, inducing a dramatic dissolution of Si by alkaline etching and *iii*) overoxidation of Si may inhibit charge transfer

from Si to catalyst. For that reason, the focus should be placed on alternative strategies allowing the use of thicker and denser coatings. In this frame, hydrothermal deposition may be useful.[65] Structured surfaces possess high surface defects which often affect the overall efficiency of Si photoelectrodes. Hence, the study of wet defect passivation strategies compatible with operation in aqueous media could be beneficial for increasing the photoelectrode performance. Efforts should also be concentrated on the elaboration of specific coating to enhance photovoltage and on the chemical protection of Si using elaborated electrolytes that can provide stability.

Supporting Information.

Extended introduction section including additional references.

AUTHOR INFORMATION

Corresponding Authors

*bruno.fabre@univ-rennes1.fr

*gabriel.loget@cnrs.fr

Author Contributions

B.F. and G.L. elaborated the plan of this Account jointly and co-wrote the manuscript.

Biographies

Bruno Fabre is, since 2008, Directeur de Recherche at CNRS. He earned his engineering diploma from the Ecole Nationale Supérieure d'Electrochimie et d'Electrométallurgie de Grenoble, France in 1990 and received his Ph.D. in Chemistry from the University of

Grenoble in 1994. In 2002, he spent one year as an invited researcher (NATO fellowship) at the National Research Council of Canada, Ottawa. His current research interests are the functionalization of surfaces, and the development of functionalized semiconducting photoelectrodes for light-activated molecular electronics and energy purposes.

Gabriel Loget is a CNRS researcher. He received his Ph.D. in Physical Chemistry from the University of Bordeaux. In 2012, he received the silver medal of the European Young Chemist Award. After that, he did a postdoctoral fellowship at the University of California, Irvine. In 2014, he was awarded an Alexander-von-Humboldt postdoctoral fellowship to conduct his research at Friedrich-Alexander Universität, Erlangen-Nürnberg. In 2015, he joined the CNRS. His current fields of interest are photoelectrochemical energy conversion and light conversion.

Funding Sources

This work has been supported by ANR (projects EASi-NANO, ANR-16-CE09-0001-01; CHALCO-CAT, ANR-15-CE06-0002-01) and by the Fondation Grand Ouest.

References

(1) Sun, K.; Shen, S.; Liang, Y.; Burrows, P. E.; Mao, S. S.; Wang, D. Enabling Silicon for Solar-Fuel Production. *Chem. Rev.* **2014**, *114* (17), 8662–8719.

(2) Torralba-Peñalver, E.; Luo, Y.; Compain, J.-D.; Chardon-Noblat, S.; Fabre, B. Selective Catalytic Electroreduction of CO_2 at Silicon Nanowires (SiNWs) Photocathodes Using Non-Noble Metal-Based Manganese Carbonyl Bipyridyl Molecular Catalysts in Solution and Grafted onto SiNWs. *ACS Catal.* **2015**, *5* (10), 6138–6147.

(3) Oh, K.; Joanny, L.; Gouttefangeas, F.; Fabre, B.; Dorcet, V.; Lassalle-Kaiser, B.; Vacher, A.; Mériadec, C.; Ababou-Girard, S.; Loget, G. Black Silicon Photoanodes Entirely Prepared with Abundant Materials by Low-Cost Wet Methods. *ACS Appl. Energy Mater.* **2019**, *2* (2), 1006–1010.

(4) Oh, K.; Dorcet, V.; Fabre, B.; Loget, G. Dissociating Water at N- Si Photoanodes Partially Covered with Fe Catalysts. *Adv. Energy Mater.* **2020**, *10* (3), 1902963.

(5) Loget, G.; Vacher, A.; Fabre, B.; Gouttefangeas, F.; Joanny, L.; Dorcet, V. Enhancing Light Trapping of Macroporous Silicon by Alkaline Etching: Application for the Fabrication of Black Si Nanospike Arrays. *Mater. Chem. Front.* **2017**, *1*, 1881–1887.

(6) Fabre, B.; Hennous, L.; Ababou-Girard, S.; Meriadec, C. Electroless Patterned Assembly of Metal Nanoparticles on Hydrogen-Terminated Silicon Surfaces for Applications in Photoelectrocatalysis. *ACS Appl. Mater. Interfaces* **2013**, *5* (2), 338–343.

(7) Dominey, R. N.; Lewis, N. S.; Bruce, J. A.; Bookbinder, D. C.; Wrighton, M. S. Improvement of Photoelectrochemical Hydrogen Generation by Surface Modification

of P-Type Silicon Semiconductor Photocathodes. *J. Am. Chem. Soc.* **1982**, *104* (2), 467–482.

(8) McKone, J. R.; Warren, E. L.; Bierman, M. J.; Boettcher, S. W.; Brunschwig, B. S.; Lewis, N. S.; Gray, H. B. Evaluation of Pt, Ni, and Ni-Mo Electrocatalysts for Hydrogen Evolution on Crystalline Si Electrodes. *Energy Environ. Sci.* **2011**, *4* (9), 3573–3583.

(9) Nunez, P.; Cabán-Acevedo, M.; Yu, W.; Richter, M. H.; Kennedy, K.; Villarino, A. M.; Brunschwig, B. S.; Lewis, N. S. Origin of the Electrical Barrier in Electrolessly Deposited Platinum Nanoparticles on P-Si Surfaces. *J. Phys. Chem. C* **2021**, *125* (32), 17660–17670.

(10) Oh, I.; Kye, J.; Hwang, S. Enhanced Photoelectrochemical Hydrogen Production from Silicon Nanowire Array Photocathode. *Nano Lett.* **2012**, *12* (1), 298–302.

(11) Fabre, B.; Li, G.; Gouttefangeas, F.; Joanny, L.; Loget, G. Tuning the Photoelectrocatalytic Hydrogen Evolution of Pt-Decorated Silicon Photocathodes by the Temperature and Time of Electroless Pt Deposition. *Langmuir* **2016**, *32* (45), 11728–11735.

(12) Hu, Y.; Chen, F.; Ding, P.; Yang, H.; Chen, J.; Zha, C.; Li, Y. Designing Effective Si/Ag Interface via Controlled Chemical Etching for Photoelectrochemical CO_2 Reduction. *J. Mater. Chem. A* **2018**, *6* (44), 21906–21912.

(13) Wei, L.; Lin, J.; Xie, S.; Ma, W.; Zhang, Q.; Shen, Z.; Wang, Y. Photoelectrocatalytic Reduction of CO_2 to Syngas over Ag Nanoparticle Modified P-Si Nanowire Arrays. *Nanoscale* **2019**, *11* (26), 12530–12536.

(14) Wang, B.; Yao, L.; Xu, G.; Zhang, X.; Wang, D.; Shu, X.; Lv, J.; Wu, Y.-C. Highly

Efficient Photoelectrochemical Synthesis of Ammonia Using Plasmon-Enhanced Black Silicon under Ambient Conditions. *ACS Appl. Mater. Interfaces* **2020**, *12* (18), 20376–20382.

(15) Huang, Z.; Chen, Z.; Chen, Z.; Lv, C.; Meng, H.; Zhang, C. $Ni_{12}P_5$ Nanoparticles as an Efficient Catalyst for Hydrogen Generation via Electrolysis and Photoelectrolysis. *ACS Nano* **2014**, *8* (8), 8121–8129.

(16) Tran, P. D.; Pramana, S. S.; Kale, V. S.; Nguyen, M.; Chiam, S. Y.; Batabyal, S. K.; Wong, L. H.; Barber, J.; Loo, J. Novel Assembly of an MoS_2 Electrocatalyst onto a Silicon Nanowire Array Electrode to Construct a Photocathode Composed of Elements Abundant on the Earth for Hydrogen Generation. *Chem. – A Eur. J.* **2012**, *18* (44), 13994–13999.

(17) Hou, Y.; Abrams, B. L.; Vesborg, P. C. K.; Björketun, M. E.; Herbst, K.; Bech, L.; Setti, A. M.; Damsgaard, C. D.; Pedersen, T.; Hansen, O.; Rossmeisl, J.; Dahl, S.; Nørskov, J. K.; Chorkendorff, I. Bioinspired Molecular Co-Catalysts Bonded to a Silicon Photocathode for Solar Hydrogen Evolution. *Nat. Mater.* **2011**, *10* (6), 434–438.

(18) Truong, T.-G.; Meriadec, C.; Fabre, B.; Bergamini, J.-F.; de Sagazan, O.; Ababou-Girard, S.; Loget, G. Spontaneous Decoration of Silicon Surfaces with MoO_x Nanoparticles for the Sunlight-Assisted Hydrogen Evolution Reaction. *Nanoscale* **2017**, *9* (5), 1799–1804.

(19) Fu, D.; Fabre, B.; Loget, G.; Mériadec, C.; Ababou-Girard, S.; Cadot, E.; Leclerc-Laronze, N.; Marrot, J.; de Ponfilly, Q. Polyoxothiometalate-Derivatized Silicon Photocathodes for Sunlight-Driven Hydrogen Evolution Reaction. *ACS Omega* **2018**, *3* (10), 13837–13849.

(20) Tourneur, J.; Fabre, B.; Loget, G.; Vacher, A.; Mériadec, C.; Ababou-Girard, S.; Gouttefangeas, F.; Joanny, L.; Cadot, E.; Haouas, M.; Leclerc-Laronze, N.; Falaise, C.; Guillon, E. Molecular and Material Engineering of Photocathodes Derivatized with Polyoxometalate-Supported $\{Mo_3S_4\}$ HER Catalysts. *J. Am. Chem. Soc.* **2019**, *141* (30), 11954–11962.

(21) Gong, Q.; Ding, P.; Xu, M.; Zhu, X.; Wang, M.; Deng, J.; Ma, Q.; Han, N.; Zhu, Y.; Lu, J.; Feng, Z.; Li, Y.; Zhou, W.; Li, Y. Structural Defects on Converted Bismuth Oxide Nanotubes Enable Highly Active Electrocatalysis of Carbon Dioxide Reduction. *Nat. Commun.* **2019**, *10* (1), 2807.

(22) Fu, D.; Tourneur, J.; Fabre, B.; Loget, G.; Lou, Y.; Geneste, F.; Ababou-Girard, S.; Mériadec, C. Bismuth-Decorated Silicon Photocathodes for CO_2-to-Formate Solar-Driven Conversion. *ChemCatChem* **2020**, *12* (22), 5819–5825.

(23) Choi, S. K.; Kang, U.; Lee, S.; Ham, D. J.; Ji, S. M.; Park, H. Sn-Coupled p-Si Nanowire Arrays for Solar Formate Production from CO_2. *Adv. Energy Mater.* **2014**, *4* (11), 1301614.

(24) Seo, J.; Pekarek, R. T.; Rose, M. J. Photoelectrochemical Operation of a Surface-Bound, Nickel-Phosphine H_2 Evolution Catalyst on p-Si(111): A Molecular Semiconductor|catalyst Construct. *Chem. Commun.* **2015**, *51* (68), 13264–13267.

(25) Gurrentz, J. M.; Rose, M. J. Non-Catalytic Benefits of Ni(II) Binding to an Si(111)-PNP Construct for Photoelectrochemical Hydrogen Evolution Reaction: Metal Ion Induced Flat Band Potential Modulation. *J. Am. Chem. Soc.* **2020**, *142* (12), 5657–5667.

(26) Hanna, C. M.; Pekarek, R. T.; Miller, E. M.; Yang, J. Y.; Neale, N. R. Decoupling

Kinetics and Thermodynamics of Interfacial Catalysis at a Chemically Modified Black Silicon Semiconductor Photoelectrode. *ACS Energy Lett.* **2020**, *5* (6), 1848–1855.

(27) Gulati, S.; Hietsoi, O.; Calvary, C. A.; Strain, J. M.; Pishgar, S.; Brun, H. C.; Grapperhaus, C. A.; Buchanan, R. M.; Spurgeon, J. M. Photocatalytic Hydrogen Evolution on Si Photocathodes Modified with Bis(Thiosemicarbazonato)Nickel(II)/Nafion. *Chem. Commun.* **2019**, *55* (64), 9440–9443.

(28) Reece, S. Y.; Hamel, J. A.; Sung, K.; Jarvi, T. D.; Esswein, A. J.; Pijpers, J. J. H.; Nocera, D. G. Wireless Solar Water Splitting Using Silicon-Based Semiconductors and Earth-Abundant Catalysts. *Science* **2011**, *334* (6056), 645–648.

(29) McCrory, C. C. L.; Jung, S.; Ferrer, I. M.; Chatman, S. M.; Peters, J. C.; Jaramillo, T. F. Benchmarking Hydrogen Evolving Reaction and Oxygen Evolving Reaction Electrocatalysts for Solar Water Splitting Devices. *J. Am. Chem. Soc.* **2015**, *137* (13), 4347–4357.

(30) Bae, D.; Seger, B.; Vesborg, P. C. K.; Hansen, O.; Chorkendorff, I. Strategies for Stable Water Splitting via Protected Photoelectrodes. *Chem. Soc. Rev.* **2017**, *46* (7), 1933–1954.

(31) Luo, Z.; Wang, T.; Gong, J. Single-Crystal Silicon-Based Electrodes for Unbiased Solar Water Splitting: Current Status and Prospects. *Chem. Soc. Rev.* **2019**, *48* (7), 2158–2181.

(32) Lee, S. A.; Choi, S.; Kim, C.; Yang, J. W.; Kim, S. Y.; Jang, H. W. Si-Based Water Oxidation Photoanodes Conjugated with Earth-Abundant Transition Metal-Based Catalysts. *ACS Mater. Lett.* **2020**, *2* (1), 107–126.

(33) Li, Y.; Xiao, Y.; Wu, C.; Zhang, D.; Huang, J.; Zhang, Z.; He, J.; Li, C. Strategies To Construct N-Type Si-Based Heterojunctions for Photoelectrochemical Water Oxidation. *ACS Mater. Lett.* **2022**, 779–804.

(34) Chen, Y. W.; Prange, J. D.; Dühnen, S.; Park, Y.; Gunji, M.; Chidsey, C. E. D.; McIntyre, P. C. Atomic Layer-Deposited Tunnel Oxide Stabilizes Silicon Photoanodes for Water Oxidation. *Nat. Mater.* **2011**, *10* (7), 539–544.

(35) Yang, J.; Walczak, K.; Anzenberg, E.; Toma, F. M.; Yuan, G.; Beeman, J.; Schwartzberg, A.; Lin, Y.; Hettick, M.; Javey, A.; Ager, J. W.; Yano, J.; Frei, H.; Sharp, I. D. Efficient and Sustained Photoelectrochemical Water Oxidation by Cobalt Oxide/Silicon Photoanodes with Nanotextured Interfaces. *J. Am. Chem. Soc.* **2014**, *136* (17), 6191–6194.

(36) Sun, K.; McDowell, M. T.; Nielander, A. C.; Hu, S.; Shaner, M. R.; Yang, F.; Brunschwig, B. S.; Lewis, N. S. Stable Solar-Driven Water Oxidation to O_2(g) by Ni-Oxide-Coated Silicon Photoanodes. *J. Phys. Chem. Lett.* **2015**, *6* (4), 592–598.

(37) Kenney, M. J.; Gong, M.; Li, Y.; Wu, J. Z.; Feng, J.; Lanza, M.; Dai, H. High-Performance Silicon Photoanodes Passivated with Ultrathin Nickel Films for Water Oxidation. *Science* **2013**, *342* (6160), 836–840.

(38) Hill, J. C.; Landers, A. T.; Switzer, J. A. An Electrodeposited Inhomogeneous Metal-Insulator-Semiconductor Junction for Efficient Photoelectrochemical Water Oxidation. *Nat. Mater.* **2015**, *14* (11), 1150–1155.

(39) Loget, G.; Fabre, B.; Fryars, S.; Mériadec, C.; Ababou-Girard, S. Dispersed Ni Nanoparticles Stabilize Silicon Photoanodes for Efficient and Inexpensive Sunlight-Assisted Water Oxidation. *ACS Energy Lett.* **2017**, *2* (3), 569–573.

(40) Oh, K.; Mériadec, C.; Lassalle-Kaiser, B.; Dorcet, V.; Fabre, B.; Ababou-Girard, S.; Joanny, L.; Gouttefangeas, F.; Loget, G. Elucidating the Performance and Unexpected Stability of Partially Coated Water-Splitting Silicon Photoanodes. *Energy Environ. Sci.* **2018**, *11* (9), 2590–2599.

(41) Stevens, M. B.; Enman, L. J.; Batchellor, A. S.; Cosby, M. R.; Vise, A. E.; Trang, C. D. M.; Boettcher, S. W. Measurement Techniques for the Study of Thin Film Heterogeneous Water Oxidation Electrocatalysts. *Chem. Mater.* **2017**, *29* (1), 120–140.

(42) Lee, S. A.; Lee, T. H.; Kim, C.; Lee, M. G.; Choi, M.-J.; Park, H.; Choi, S.; Oh, J.; Jang, H. W. Tailored NiO_x/Ni Cocatalysts on Silicon for Highly Efficient Water Splitting Photoanodes via Pulsed Electrodeposition. *ACS Catal.* **2018**, *8*, 7261–7269.

(43) Tung, C. W.; Chuang, Y.; Chen, H. C.; Chan, T. S.; Li, J. Y.; Chen, H. M. Tunable Electrodeposition of Ni Electrocatalysts onto Si Microwires Array for Photoelectrochemical Water Oxidation. *Part. Part. Syst. Charact.* **2018**, *35* (1), 1–8.

(44) Zhao, J.; Gill, T. M.; Zheng, X. Enabling Silicon Photoanodes for Efficient Solar Water Splitting by Electroless-Deposited Nickel. *Nano Res.* **2018**, *11* (6), 3499–3508.

(45) Laskowski, F. A. L.; Oener, S. Z.; Nellist, M. R.; Gordon, A. M.; Bain, D. C.; Fehrs, J. L.; Boettcher, S. W. Nanoscale Semiconductor/Catalyst Interfaces in Photoelectrochemistry. *Nat. Mater.* **2020**, *19* (1), 69–76.

(46) Lee, S. A.; Lee, T. H.; Kim, C.; Choi, M.-J.; Park, H.; Choi, S.; Lee, J.; Oh, J.; Kim, S. Y.; Jang, H. W. Amorphous Cobalt Oxide Nanowalls as Catalyst and Protection Layers on N-Type Silicon for Efficient Photoelectrochemical Water Oxidation. *ACS Catal.* **2020**, *10* (1), 420–429.

(47) Li, F.; Li, Y.; Zhuo, Q.; Zhou, D.; Zhao, Y.; Zhao, Z.; Wu, X.; Shan, Y.; Sun, L.

Electroless Plating of NiFeP Alloy on the Surface of Silicon Photoanode for Efficient Photoelectrochemical Water Oxidation. *ACS Appl. Mater. Interfaces* **2020**, *12* (10), 11479–11488.

(48) Xu, G.; Xu, Z.; Shi, Z.; Pei, L.; Yan, S.; Gu, Z.; Zou, Z. Silicon Photoanodes Partially Covered by Ni@$Ni(OH)_2$ Core–Shell Particles for Photoelectrochemical Water Oxidation. *ChemSusChem* **2017**, *10*, 2897 –2903.

(49) Chen, J.; Xu, G.; Wang, C.; Zhu, K.; Wang, H.; Yan, S.; Yu, Z.; Zou, Z. High-Performance and Stable Silicon Photoanode Modified by Crystalline Ni@ Amorphous Co Core-Shell Nanoparticles. *ChemCatChem* **2018**, *10* (21), 5025–5031.

(50) Cai, Q.; Hong, W.; Jian, C.; Liu, W. A High-Performance Silicon Photoanode Enabled by Oxygen Vacancy Modulation on NiOOH Electrocatalyst for Water Oxidation. *Nanoscale* **2020**, *12* (14), 7550–7556.

(51) Lee, S. A.; Park, I. J.; Yang, J. W.; Park, J.; Lee, T. H.; Kim, C.; Moon, J.; Kim, J. Y.; Jang, H. W. Electrodeposited Heterogeneous Nickel-Based Catalysts on Silicon for Efficient Sunlight-Assisted Water Splitting. *Cell Rep. Phys. Sci.* **2020**, *1* (10), 100219.

(52) Loget, G.; Mériadec, C.; Dorcet, V.; Fabre, B.; Vacher, A.; Fryars, S.; Ababou-Girard, S. Tailoring the Photoelectrochemistry of Catalytic Metal-Insulator-Semiconductor (MIS) Photoanodes by a Dissolution Method. *Nat. Commun.* **2019**, *10* (1), 3522.

(53) Laskowski, F. A. L.; Nellist, M. R.; Venkatkarthick, R.; Boettcher, S. W. Junction Behavior of N-Si Photoanodes Protected by Thin Ni Elucidated from Dual Working Electrode Photoelectrochemistry. *Energy Environ. Sci.* **2017**, *10* (2), 570–579.

(54) Loget, G. Water Oxidation with Inhomogeneous Metal-Silicon Interfaces. *Curr. Opin. Colloid Interface Sci.* **2019**, *39*, 40–50.

(55) Hemmerling, J. R.; Mathur, A.; Linic, S. Characterizing the Geometry and Quantifying the Impact of Nanoscopic Electrocatalyst/Semiconductor Interfaces under Solar Water Splitting Conditions. *Adv. Energy Mater.* **2022**, *12* (11), 2103798.

(56) Tung, C.-W.; Kuo, T.-R.; Hsu, C.-S.; Chuang, Y.; Chen, H.-C.; Chang, C.-K.; Chien, C.-Y.; Lu, Y.-J.; Chan, T.-S.; Lee, J.-F.; Li, J.-Y.; Chen, H. M. Light-Induced Activation of Adaptive Junction for Efficient Solar-Driven Oxygen Evolution: In Situ Unraveling the Interfacial Metal–Silicon Junction. *Adv. Energy Mater.* **2019**, *9* (31), 1901308.

(57) Tung, R. T. The Physics and Chemistry of the Schottky Barrier Height. *App. Phys. Rev.* **2014**, *1*, 011304.

(58) Rossi, R. C.; Lewis, N. S. Investigation of the Size-Scaling Behavior of Spatially Nonuniform Barrier Height Contacts to Semiconductor Surfaces Using Ordered Nanometer-Scale Nickel Arrays on Silicon Electrodes. *J. Phys. Chem. B* **2001**, *105* (49), 12303–12318.

(59) Aroonratsameruang, P.; Pattanasattayavong, P.; Dorcet, V.; Mériadec, C.; Ababou-Girard, S.; Fryars, S.; Loget, G. Structure–Property Relationships in Redox-Derivatized Metal–Insulator–Semiconductor (MIS) Photoanodes. *J. Phys. Chem. C* **2020**, *124* (47), 25907–25916.

(60) Dong, W. J.; Song, Y. J.; Yoon, H.; Jung, G. H.; Kim, K.; Kim, S.; Lee, J.-L. Monolithic Photoassisted Water Splitting Device Using Anodized Ni-Fe Oxygen Evolution Catalytic Substrate. *Adv. Energy Mater.* **2017**, *7* (19), 1700659.

(61) Oh, K.; de Sagazan, O.; Léon, C.; Le Gall, S.; Loget, G. Custom Plating of Nanoscale Semiconductor/Catalyst Junctions for Photoelectrochemical Water Splitting. *Nanoscale*

2021, *13*, 1997–2004.

(62) Menke, E. J.; Thompson, M. A.; Xiang, C.; Yang, L. C.; Penner, R. M. Lithographically Patterned Nanowire Electrodeposition. *Nat. Mater.* **2006**, *5* (11), 914–919.

(63) Fabre, B. Functionalization of Oxide-Free Silicon Surfaces with Redox-Active Assemblies. *Chem. Rev.* **2016**, *116* (8), 4808–4849.

(64) Kasemthaveechok, S.; Oh, K.; Fabre, B.; Bergamini, J.-F.; Mériadec, C.; Ababou-Girard, S.; Loget, G. A General Concept for Solar Water-Splitting Monolithic Photoelectrochemical Cells Based on Earth-Abundant Materials and a Low-Cost Photovoltaic Panel. *Adv. Sustain. Syst.* **2018**, *2* (11), 1800075.

(65) Dabboussi, J.; Abdallah, R.; Santinacci, L.; Zanna, S.; Vacher, A.; Dorcet, V.; Fryars, S.; Floner, D.; Loget, G. Solar-Assisted Urea Oxidation at Silicon Photoanodes Promoted by an Amorphous and Optically Adaptive Ni-Mo-O Catalytic Layer. *J. Mater. Chem. A* **2022**, 10, 19769–19776.